# Experimental measurements of sidebranching in thermal dendrites under terrestrial-gravity and microgravity conditions

D. P. Corrigan, M. B. Koss, J. C. LaCombe, K. D. de Jager, L. A. Tennenhouse, and M. E. Glicksman
*Materials Science and Engineering Department, Rensselaer Polytechnic Institute, Troy, New York 12180-3590*
(Received 27 July 1999)

We perform sidebranch measurements on pure succinonitrile dendrites grown in both microgravity and terrestrial-gravity conditions for a set of supercoolings within the range 0.1–1.0 K. Two distinct types of sidebranch regions, uniform and coarsening, exist, and are characterized by the distance from the tip at which the region began, $D_i$, and the average spacing of sidebranches within that region, $\lambda_i$. There does not appear to be any significant dependence on either gravity level or supercooling when $D_i$ or $\lambda_i$ are normalized with respect to the radius of curvature of the tip, $R$. The apparently constant normalized proportionality factor between $D_i$, $\lambda_i$, and $R$, regardless of the relative importance of diffusion and convective heat transport, demonstrates self-similarity between dendrites of different length scales propagating under various heat transfer conditions. However, when the form of the sidebranch envelope is defined by a power law relating the amplitude and relative positions of the sidebranches normalized to the radius of the tip, the form is seen to have significant variations with supercooling between the terrestrial gravity and microgravity growth dendrites. Furthermore, both the amplitude coefficient and exponent from the power-law regressions of the microgravity data are statistically different (95% confidence level) than their terrestrial counterparts.
[S1063-651X(99)11612-X]

PACS number(s): 68.70.+w, 81.10.Mx, 81.30.Fb

## I. INTRODUCTION

Morphologically complex solidification microstructures, such as dendrites, appear in a large number of common engineering materials in which the existing thermal and solutal fields within the melt provide the necessary physical conditions for the advancement of a morphologically unstable solid-liquid interface. If the solidification conditions fall within a regime of low thermal gradients and low crystalline anisotropy, then dendrites form as dictated by heat transport within the system and capillary effects at the solid-melt interface. Solidification environments that provide the necessary conditions for dendritic morphologies are often encountered in typical metallurgical processes, such as casting and welding. Consequently, it is necessary to understand the basic process of dendritic growth in order to improve processing conditions for optimization of solidification microstructures. More importantly, it is essential to understand the process of dendritic sidebranch growth, because in most commonly utilized structural engineering materials, the evolution of sidebranches ultimately segregates solute into its final distribution, dictating in part the mechanical, electrical, and chemical properties of the as-solidified material. Therefore, in order to relate the microstructural features within a given material to its macrostructural properties, it is first necessary to comprehend the physics underlying the complex process of sidebranch evolution.

## II. BACKGROUND

At the steady state, the primary tip of the dendrite may be defined by two measurable parameters, namely, the radius of curvature at the tip, $R$, and its growth velocity $V$. Unique predictions of these two measurables, by both current theories of dendrite growth, and large-scale numerical simulations of dendritic growth, are usually comprised of two independent components. The first concerns the transport of heat and solute from the solid-liquid interface into the melt. The second involves the interfacial physics, which complements the heat transport, and selects the unique growth rate and tip radius of curvature from a manifold of solutions that satisfy the heat transfer and conservation of energy at the solid-melt interface. Full discussions of the theoretical and experimental developments of dendritic growth are found in Langer's review article [1], Pelce's book [2], and Glicksman and Marsh's review article [3]. There are also introductions in the recent articles by Juric and Tryggvason [4], and Bisang and Bilgram [5], although not recent enough to include the latest developments in three-dimensional or adaptive grid phase field modeling.

Until recently, neither the heat transfer nor the interfacial selection aspects of theory could be tested critically on the Earth because of the effects of gravity-induced convection, which modifies the transport processes and alters the growth kinetics [6]. Several of the authors of this paper obtained benchmark data on dendritic growth using succinonitrile (SCN) in a microgravity environment where convective effects were essentially eliminated [7–9]. The data and subsequent analysis of the dendritic tip growth speed $V$ and radii of curvature at the dendrite tip, $R$, demonstrated that although basic theory yields predictions that are reasonably in agreement with the results of experiment, several significant discrepancies occur [10]. Some of the discrepancies can be understood by a careful consideration of the diffusion of heat from complex three-dimensional dendritic structures [11]. The data and analysis for assessing the interfacial physics are less definitive.

Key to the evaluation of the transport physics was the analysis of the effect of latent heat generation in the sidebranch region beyond ~12 tip radii behind the tip. Dendritic

 

sidebranches are also intimately related to the interfacial selection rules, as the same physics that initiates and supports sidebranch formation is the source of the interfacial selection or scaling rule. Thus a complete theory or simulation of dendritic growth must include sidebranches, and experiments that describe dendritic growth must characterize dendritic sidebranching in addition to the measurements of tip velocity and radius of curvature. In this paper, after a brief background and literature review, we present a detailed examination of dendritic sidebranching characteristics of the benchmark SCN microgravity data.

One way to quantify the sidebranch structure is by measuring the sidebranch spacing $\lambda$, which is the distance perpendicularly between adjacent sidebranches. Sidebranch spacing is an easily identifiable and quantifiable parameter, which defines the characteristics of a particular dendrite. It also adds important information about the final microstructure, which governs the properties of the material. It has been determined empirically that a linear scaling relationship exists between the sidebranch spacing and the radius of curvature of the dendrite tip. Moreover, this scaling relation remains constant over a wide range of supercoolings. For instance, a study conducted by Hürlimann *et al.* [12] on xenon dendrites revealed that, independent of supercooling, sidebranches in close proximity to the tip tend to grow with a characteristic spacing of $\lambda_s/R=3.2\pm0.4$. Pinus and Taylor [13] conducted a similar study of SCN, and determined that a similar scaling relationship exists with $\lambda_s/R=2.9\pm0.3$. Experiments on SCN by Glicksman and Huang [14] also revealed a comparable scaling law independent of supercooling with $\lambda_s/R=2-5$. The measurements made in these investigations were on sidebranches close to the tip, in a region where the thermal fields surrounding the sidebranches interact relatively weakly. A more developed and stronger interaction of thermal fields occurs between adjacent sidebranches that are further behind the tip, resulting in coarsening. Coarsening is a process governed by capillarity in which sidebranches with higher curvatures tend to remelt, benefitting sidebranches with smaller curvatures. This coarsening region is preferentially located many radii behind the tip, due to the fact that the thermal boundary layers for these remote sidebranches have more time to grow and interact than the newly created interfacial regions near the tip. Due to this coarsening process, there is larger variability in the sidebranch spacing in the coarsening region compared to that seen in the more uniformly spaced region located closer to the tip. This investigation will quantify the existence of sidebranch scaling relationships in both the near-tip and coarsening regions, since both are observed experimentally and have a significant impact on the resulting microstructure.

Several solidification models, including stagnant film models [15] and mesoscopic numerical simulations [16], define a hypothetical ''grain envelope'' that defines the bounding surface for the macroscopic heat flux generated by a single equiaxed dendrite. A grain envelope is prescribed by delineating the common smooth surface connecting the tips of all the sidebranches and the primary tip. To provide useful information for use in these models, it is the purpose of the present investigation to quantify the mathematical nature of this dendrite envelope and to expose any scaling relationships that potentially may exist within its shape. These scaling relationships are phenomenological and represent an attempt to assign a simple, quantifiable parameter to a complex process.

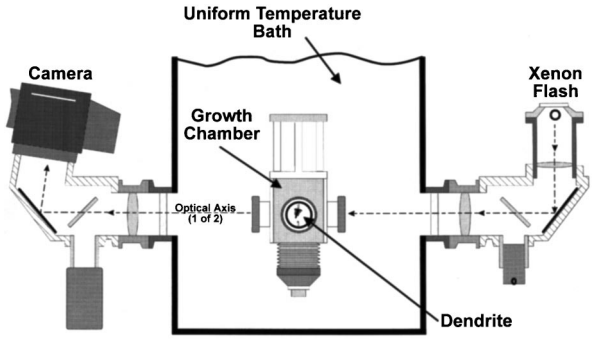


FIG. 1. Schematic of IDGE growth chamber and temperature control bath used for the growth and optical observation of dendritic growth.

The assumption that the process of conduction regulates the transport of heat, is common to the theories describing sidebranch evolution (for example, see Refs. [17–21]). As stated earlier, in any experiment conducted terrestrially, the presence of gravity creates buoyancy-driven convective heat transport due to the interaction of the gravitational field with the thermally induced density gradients within the liquid. This additional mode of heat transport in most cases dominates the effects of diffusion. As a consequence, convection can complicate the assessment of the majority of theoretical analyses that do not account for it. The main purpose of this study is to characterize dendritic sidebranch structure by altering the heat transport conditions through controlled changes in the magnitude of gravity and supercooling.

## III. EXPERIMENTAL APPARATUS AND PROCEDURE

In March of 1994, the first of several planned flights of the isothermal dendritic growth experiment (IDGE) took place aboard the space shuttle Columbia (STS-62). The apparatus used to grow pure succinonitrile dendrites orbited the earth aboard the United States Microgravity Payload-2, in a high-quality microgravity environment for 11 days, thereby allowing dendritic growth with diffusion-limited heat transport. The same apparatus was used terrestrially to obtain an Earth-based counterpart to the microgravity data. In microgravity, 58 dendrite growth cycles were performed at supercoolings ranging from 0.1 to 1.0 K. Reference [10] details the microgravity experiment; however, for completeness, we give a brief outline of the experimental procedures.

The experiments conducted in this investigation were performed using pure SCN [chemical formula NC-$(CH_2)_2$-CN, purity $\sim$99.999%] in a stainless steel and borosilicate glass growth chamber surrounded by a temperature bath controlled to $\pm0.002$ K. A detailed schematic of the IDGE growth chamber is shown in Fig. 1. SCN is an ideal material for conducting solidification experiments because of its low melting point (58 °C), optical transparency, and metal-like solidification characteristics. The process for growing a dendrite is initiated by first melting the SCN within the chamber, and lowering the temperature of the bath to the desired supercooling. Then, after the SCN has stabilized at the speci-

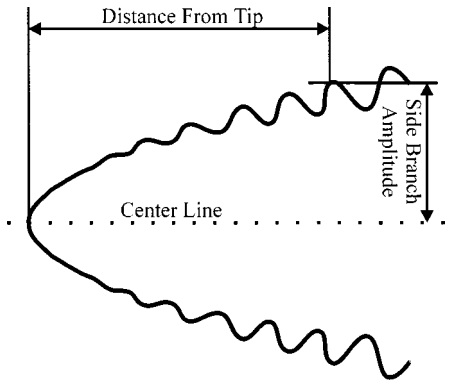


FIG. 2. Geometrical method used to measure the sidebranch amplitude and position. The coordinate system has an origin situated at the tip of the dendrite and, thus, moves with respect to the laboratory frame of reference. That is, the coordinate system remains fixed with respect to the dendrite tip.

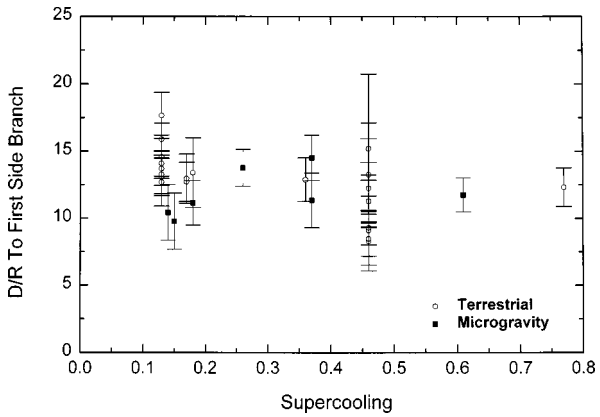


FIG. 3. Plot of the distance to the first detectable sidebranch scaled by the tip radius for various supercoolings. Over a large range of supercoolings, this dimensionless parameter describing the nature of the sidebranching is relatively constant.

fied temperature, a thermoelectric cooler located at the top of a nucleation tube (the ''stinger'') is activated. After nucleation of the dendrite crystal at the top of the stinger, the dendrite propagates along the length of the tube until it emerges in the main volume of the supercooled SCN melt. After attaining steady state growth, 35-mm photographs are taken from perpendicular views at predefined time intervals. These images characterize the dendritic growth process, from which the growth velocity, tip radius, and sidebranch information are extracted.

The 35-mm IDGE negatives are analyzed using a microscope-vernier arrangement to determine the interface shape, sidebranch information, and growth velocity vector, for each dendrite [22]. An image capture system is used to locate the edge of the dendrite to produce a set of $(x,y)$ coordinate pairs representing the solid-liquid interface. A fourth-order polynomial fitting function is then regressed to this data set in order to determine the radius of curvature of the tip. This process was previously described by LaCombe *et al.* [23] and Koss *et al.* [10].

Sidebranch spacing and amplitude are measured with respect to the axial centerline of the dendrite, as depicted in Fig. 2. The first observable sidebranch is defined as the first protrusion from the dendrite tip that can be measured using the vernier-oscilloscope measuring apparatus. The first detectable sidebranch defines the beginning of the uniformly spaced sidebranch region. The beginning of the coarsening region is defined as the location of the first sidebranch whose amplitude is less than its neighbor in the direction of the tip. All distances between sidebranches are measured from tip-to-tip parallel to the axial centerline. Also important to note is that all measured linear distances are corrected geometrically to account for optical magnification and stereographic projection.

## IV. RESULTS AND DISCUSSION

### First detectable sidebranch

The distance to the first detectable sidebranch was measured for both the terrestrial and microgravity data for various supercoolings. For a particular growth, the distance to the first detectable sidebranch was measured via the vernier-oscilloscope measurement apparatus (described previously) in each 35-mm image. Typically there were three images per growth cycle, with measurements made on both the left and right sides of the dendrite, with the resulting values normalized using the measured tip radius. These six sequential measurements (three from each side) of the steady state dendrite are then combined to produce an average and a standard deviation. This process was repeated for various supercoolings to form the complete IDGE data set shown in Fig. 3. Within the statistical variation of this data set, defined as one standard deviation, there does not seem to be any correlation between supercooling and the scaled distance to the first sidebranch. Stated differently, if a variation with supercooling exists within the data, it is less than the statistical variation represented by the error bars. Thus it can be stated that the distance to the first sidebranch, when scaled to the radius of the tip, does not vary with supercoolings, and can be represented as

$$D_0 = C_0 R. \tag{1}$$

Here $D_0$ is the distance to the first detectable sidebranch, $C_0$ is the scaling constant, and $R$ is the measured radius of the dendrite tip. Based on analysis of the data in Fig. 3, in a terrestrial environment, $C_{0(g=1)} = 12.7 \pm 2.3$, and in microgravity, $C_{0(g=0)} = 11.8 \pm 1.7$. Using a two-tailed $t$ test with a confidence level of 95% on both data sets, and the assumption of equal variances, we conclude that the scaling constants for the microgravity and terrestrial data sets are not distinguishable.

### Distance to first detectable coarsening

The distance to the first detectable sidebranch in the coarsening region is defined as the first sidebranch encountered, when moving away from the tip, whose amplitude is less in magnitude than the previous sidebranch. This definition provides a repeatable method of accurately quantifying the scale at which the coarsening process occurs from the tip. To discern the effects of convection on the coarsening process, this analytical approach was applied to both the terrestrial and ground-based data sets using the same vernier-oscilloscope measuring apparatus. Again, this was performed

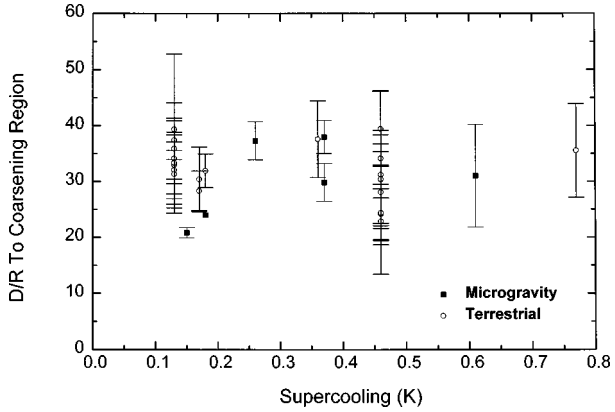


FIG. 4. Plot of the distance to the first detectable coarsening normalized by the tip radius $D_c$, vs supercooling for both terrestrial and microgravity based data. It cannot be concluded from this data whether a correlation exists between the magnitude of gravity and $D_c$. Additionally, it cannot be assumed that the magnitude of supercooling affects $D_c$ to any noticeable degree.

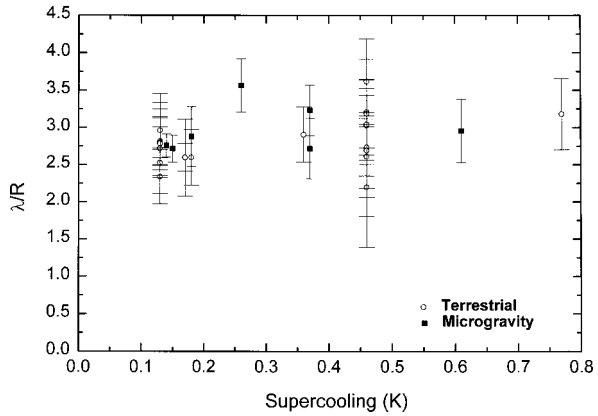


FIG. 5. Graph of the average normalized sidebranch spacing within a region extending 25 radii behind the tip. There is no statistical difference between the microgravity and terrestrial data, nor is there any significant correlation between supercooling and the normalized sidebranch spacing within this regime.

on a series of three images taken sequentially in time for a given growth for the right and left halves of the dendrite. These six measurements were averaged, also producing a corresponding standard deviation for the distance to first detectable coarsening branch for each growth. This process was repeated for different supercoolings, and resulted in the data set shown in Fig. 4. It cannot be concluded that any trend exists with supercooling for either the terrestrial or microgravity data sets to within experimental error and sample variation. If such an effect is physically present, then it is less than the standard deviation of the measurements. Again, the same type of scaling relationship can be applied to each data set, namely,

$$D_c = C_c R. \tag{2}$$

In this case, $D_c$ is the distance to the first detectable coarsening, and $C_c$ is the scaling constant. Application of Eq. (2) to the data yields a terrestrial scaling constant of $C_{c(g=1)} = 33.3 \pm 7.4$ and a microgravity scaling constant of $C_{c(g=0)} = 30.2 \pm 6.9$. Employing the $t$ test with a 95% confidence level reveals that these two scaling constants are statistically equivalent. These results support, in a statistical sense, that there is no correlation between gravity or supercooling and the scaled distance, $D_c$, to the first coarsening event.

### Sidebranch spacing in uniform regime

Sidebranch spacings scaled to the tip radius were measured for both the microgravity and terrestrial data sets within the uniform region. This region is defined as encompassing the first detectable sidebranch and the first detectable coarsening branch. As shown previously, the first detectable coarsening occurred approximately 30–33 radii behind the tip. However, to simultaneously ensure that the uniform region did not contain a coarsening event, and that it was consistent for each growth, the uniform region was defined to begin at the first detectable sidebranch, and end 25 radii behind the tip. This ensured, to a large extent, that coarsening effects were minimal in the uniform region to within one standard deviation of the coarsening region boundary at 30 radii. As earlier, a series of six measurements were combined, producing an average and a standard deviation. This was repeated for growths performed under different supercoolings, resulting in the data shown in Fig. 5. The data reveal that, to within one standard deviation, no definitive correlation exists between gravity and the average sidebranch spacing within this region. Again, all plotted error bars represent one standard deviation, and when considering the apparent constant behavior of the data throughout the entire range of supercoolings, it is statistically viable to conclude that a self-similar scaling law holds as

$$\lambda_u = C_u R. \tag{3}$$

Here $\lambda_u$ is the sidebranch spacing in the uniform region, and $C_u$ is the scaling constant. The terrestrial scaling constant for the sidebranch spacing in the uniform region is $C_{u(g=1)} = 2.81 \pm 0.31$, and in microgravity is $C_{u(g=0)} = 2.98 \pm 0.32$. To a 95% confidence level, these coefficients are statistically identical. Note that these results are in agreement with the spacings reported by Pinus and Taylor [13], in which a scaling constant of $C_{u(g=1)} = 2.9 \pm 0.30$ was reported for SCN. These data are also consistent with spacings in xenon dendrites reported by Hürlimann *et al.* [12].

### Sidebranch spacing in coarsening regime

To quantify sidebranch behavior further behind the tip where coarsening processes are more common, spacings between sidebranches in the region extending 25–50 radii behind the primary tip were evaluated for both the terrestrial and microgravity data sets. To be consistent with the average boundary defined for the uniform region at 25 radii and to maximize the number of measured sidebranches, the coarsening region was defined to begin at 25 radii behind the tip, and end 50 radii behind the tip. Statistical averaging of the data as described previously was performed for growths at various supercoolings, and is summarized in Fig. 6. Again, to within one standard deviation, the sidebranch spacing appears to be independent of the supercooling. This conclusion can be justified with either the microgravity or terrestrial data

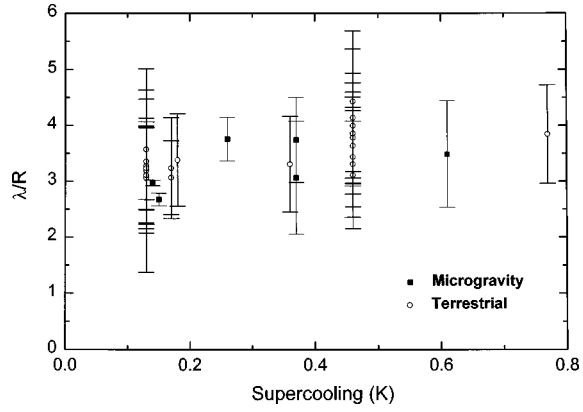


FIG. 6. Plot of the normalized sidebranch spacing averaged within a region defined between 25 and 50 radii behind the tip. In this region, a significant amount of thermal interactions between sidebranches is present. Therefore, coarsening is prevalent, manifesting itself, on average, as a larger sidebranch spacing than that obtained in the uniform region. Furthermore, a larger scatter in the data is present, due to the coarsening process in this regime. Again, no significant trend between supercooling or the magnitude of gravity is observed in these data.

sets. To express the self-similarity of sidebranches in the coarsening regime, we use the linear form

$$\lambda_{\mathrm{coar}} = C_{\mathrm{coar}} R, \tag{4}$$

where $\lambda_{\mathrm{coar}}$ is the sidebranch spacing in the coarsening regime, and $C_{\mathrm{coar}}$ is the scaling constant. Application of Eq. (4) results in a terrestrial scaling constant of $C_{\mathrm{coar}(g=1)} = 3.48 \pm 0.38$ and a microgravity scaling constant of $C_{\mathrm{coar}(g=0)} = 3.28 \pm 0.45$. Notice that both the sidebranch spacing and its variance in this region are significantly larger than they were in the uniform region due to the influence of coarsening. After performing a *t* test on these data, it can be concluded that the spacing in the coarsening region is statistically larger than the spacing in the uniform region. However, as stated above, when comparing the terrestrial and microgravity scaling constants within the coarsening region using the *t* test, it is found that these two scaling relationships are statistically identical. It can therefore be concluded that convection and supercooling have little or no effect on the normalized sidebranch spacing in the coarsening region.

### Sidebranch envelope

In order to characterize the shape of the envelope produced by the sidebranches, the approach of Dougherty and Gunawardana [24] and also of Li and Beckermann [25] was applied. Specifically, the *Z* coordinate of the sidebranch tips were linearly regressed in the form of a power law given by

$$\frac{Z}{R} = \alpha \left( \frac{X}{R} \right)^{\beta}. \tag{5}$$

Here, *Z* is the coordinate back from the tip, *X* is the orthogonal coordinate, $\alpha$ is the preexponential term, and $\beta$ is the exponential term. The coordinate system is defined such that the origin is at the tip, and the *Z* axis is aligned with the primary growth direction. Figure 7 shows an example of the

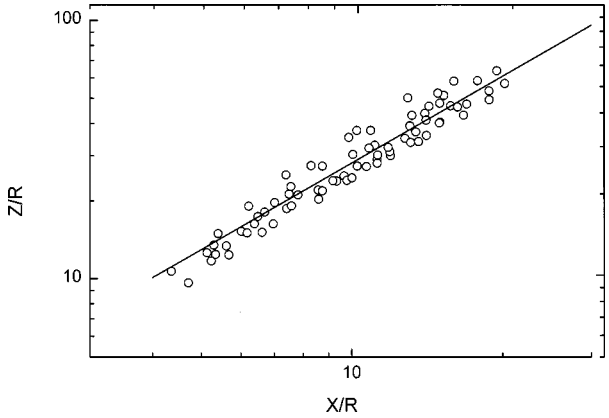


FIG. 7. When sidebranch tip positions are scaled by the radius of the tip, a power-law behavior (dotted line) accurately describes the shape of this sidebranch envelope. This regression scheme was performed on all microgravity and terrestrial data to obtain a scaling relationship that yields average values for the preexponent $\alpha$ and the exponent $\beta$.

sidebranch data from a single dendrite, along with the corresponding power-law fit. This analysis was performed for all of the photographs taken for a given growth for both the left and right halves of the dendrite (the absolute value of the *X* coordinates were taken so that the power regression could be performed). The values of $\alpha$ and $\beta$ were then averaged for each growth and plotted vs supercooling, as seen in Figs. 8 and 9. It is observed that these two scaling parameters ($\alpha$ and $\beta$) also appear to be independent of the supercooling, to within statistical dispersion, for both the microgravity and terrestrial data sets. It is important to note that this scaling invariance only occurs when the coordinates of the sidebranch tips are normalized to the radius of the tip, which simply provides a measure of the dendrite size. In this sense we observe a self-similarity for not only the spacing between sidebranches, but also for the sidebranch amplitude. Accepting the constant behavior of either of these two parameters with supercooling leads to the possible use of the parameters $\alpha$ and $\beta$ for characterizing both the microgravity and terrestrial sidebranch envelopes. This can serve as an empirical

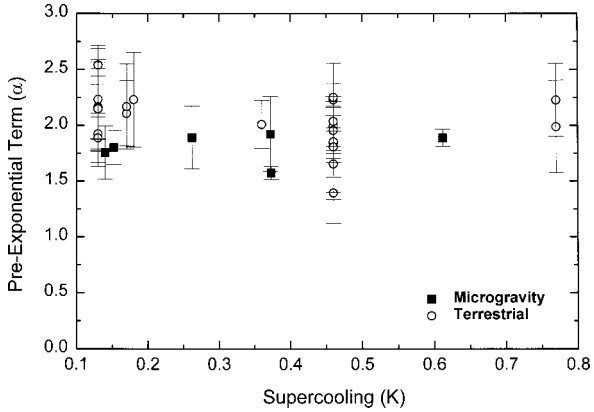


FIG. 8. Preexponent $\alpha$ for both the microgravity and terrestrial data sets, vs supercooling. From these data two significant observations can be made: (1) there is no noticeable relationship between supercooling and $\alpha$, and (2) there is a statistically significant difference between the microgravity and terrestrial preexponents.

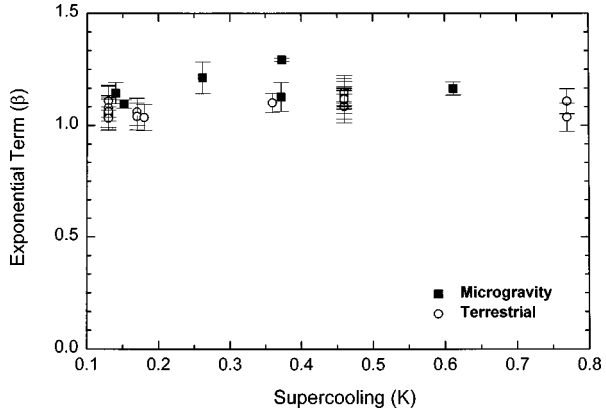


FIG. 9. Exponent $\beta$ for both the microgravity and terrestrial data sets, vs supercooling. Again, two observations can be drawn: (1) $\beta$ remains remarkably invariant to the level of supercooling, and (2) the average $\beta$ for the terrestrial data is significantly lower than the microgravity exponent.

tool to describe, in an average sense, a complex stochastic phenomenon. An analysis of this form yields a power relationship for the average microgravity envelope of the form

$$\left(\frac{Z}{R}\right)_{\text{mic}} = (1.81 \pm 0.13)\left(\frac{X}{R}\right)_{\text{mic}}^{(1.174 \pm 0.071)}. \tag{6}$$

The corresponding power relationship for the average envelope, under terrestrial conditions, takes the form

$$\left(\frac{Z}{R}\right)_{\text{terr}} = (2.04 \pm 0.23)\left(\frac{X}{R}\right)_{\text{terr}}^{(1.087 \pm 0.038)}. \tag{7}$$

Performing a two tailed $t$ test on $\alpha_{\text{mic}}$ and $\alpha_{\text{terr}}$ with a 95% level of confidence reveals that the preexponential coefficients are significantly different in these environments. Similarly, using the same $t$-test analysis, the same conclusion is drawn for $\beta_{\text{mic}}$ and $\beta_{\text{terr}}$. It is inferred from this analysis that a statistically significant difference exists in the morphology of the sidebranch envelope between dendrites growing on earth and in microgravity. Thus the modes of heat transport available to the dendritic crystal affect its sidebranch envelope shape. Interestingly, a similar conclusion cannot be drawn in either the microgravity or terrestrial data when considering only the level of supercooling, as clearly seen in Figs. 8 and 9. It is also interesting to point out that when our data from the same microgravity flight were independently analyzed by Li and Beckerman [25], a slightly different value for $\alpha_{\text{mic}}$ was obtained. Specifically, they obtained a value of $\alpha_{\text{mic}}=1.5$ (no standard deviation reported). However, their measured value of $\beta_{\text{mic}}$ was 1.164, which is almost identical to the exponent achieved by this present analysis. It is contended here that this difference in $\alpha_{\text{mic}}$ is directly a result of our method of parsing the data sets. In the present analysis, only dendrites that were growing with the sidebranch planes perpendicular to the primary arm and parallel to the projection plane were used. This eliminated the potential for a double projection of sidebranches cast from superimposed sidebranch planes. When a three-dimensional object is projected onto a two-dimensional surface, it is difficult to discern between sidebranches from one plane and those of another whose projections overlap. By parsing the data we included only those dendrites where this was not an issue. This limited the number of growths that could be analyzed, but ensured the reliability of the data. Li and Beckermann [25] did not discuss this aspect of the measurements, so how this issue was addressed is uncertain. Furthermore, only ''active'' sidebranches were included in their regression. An active sidebranch is one that is actively growing, and not shrinking due to coarsening. Our analysis included all sidebranches, both active and inactive, because in our definition these represent the true sidebranch envelope. Even though a sidebranch is ''inactive,'' it is still present and affects the thermal field and the process in general. It is not clear why Li and Beckermann excluded inactive sidebranches when attempting to quantify the shape of the actual envelope. Therefore, these two data sets cannot be reasonably compared with any level of confidence, and such a discrepancy in the coefficients can be expected as a direct consequence. For general comparison, a similar analysis of pivalic acid dendrites (another model material, with fcc structure) grown under terrestrial conditions with a 1% ethanol impurity by Dougherty and Gunawardana [24] resulted in a power law fit with $1.25<\beta_{\text{terr}}<1.67$.

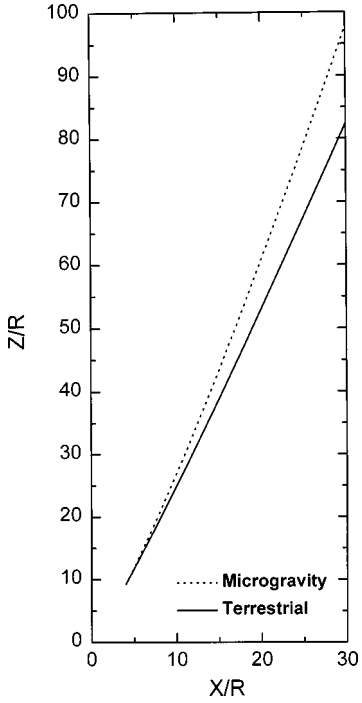


FIG. 10. The average sidebranch envelope for terrestrially grown and space-flight-grown dendrites as obtained through the power-law scaling scheme. This graph reveals that there is a significant difference between the two envelopes. More specifically, the microgravity envelope is narrower and the terrestrial envelope is wider. This observation is attributed to the interaction of gravitationally induced convection and the developing sidebranch arms.

To graphically represent the difference between the microgravity and terrestrial sidebranch envelopes, a graph of the average envelopes defined by Eqs. (6) and (7) is presented in Fig. 10. This plot indicates that in microgravity, the sidebranches possess, on average, an amplitude (scaled by the tip radius) somewhat reduced in magnitude from the terrestrial sidebranches. Although sidebranching is a complex

process, it is suggested by these measurements that this difference is real and is a direct consequence of melt-flow interactions with the sidebranches. It is further suggested that flow in the melt induced by gravity interacts with the temperature field enveloping the dendrite in such a way that perturbs the envelope shape significantly from its pure diffusive form. More importantly, one should recognize that the change in shape of the envelope is not related to changes in the sidebranch spacing because this parameter, as revealed earlier, is identical under terrestrial and microgravity conditions. Therefore, it must be concluded that the change in shape of the envelope is directly connected to a variation in sidebranch amplitude, and not to the sidebranch spacing.

## V. CONCLUSIONS

Dendritic growth experiments, conducted under both terrestrial and microgravity conditions, have led to the following conclusions with regard to the self-similarity of sidebranch parameters.

(1). To within the statistical spread in the data, no measured correlation with the magnitude of gravity or thermal supercooling exists for (a) the scaled distance to the first detectable sidebranch, (b) the scaled spacing between sidebranches in the uniform and coarsening regions, and (c) the scaled distance to the first detectable coarsening. Scaling any of these sidebranch parameters with the dendritic tip radius reveals a self-similar behavior for dendrites grown in dramatically different heat transport environments, differing by more than one order of magnitude in the supercooling, and several orders of magnitude in the thermal gradient.

(2). When measuring the sidebranch envelope, i.e., the smooth surface connecting the primary tip and the tips of the sidebranches, it is found that the shape of this surface may be described in the form of a power law. This regression scheme reveals that the power-law coefficients are invariant to the supercooling in both microgravity and terrestrial growth conditions. The observed behavior of these power-law coefficients strengthens the applicability of self-similarity and scaling laws when describing the sidebranch envelope. However, this must be approached with caution, primarily because the data reveal that the average shape of the sidebranch envelope is, in fact, sensitive to the modes of heat transport. The evidence supporting this observation is the statistical difference between the power-law coefficients for dendrites grown in microgravity versus terrestrial conditions. It is concluded that the alteration in the shape of the normalized envelope (induced by gravity) is a manifestation of sidebranch amplitude variations induced by flow field interactions, and not due to changes in the sidebranch spacing.

## ACKNOWLEDGMENTS

This work was generously supported by NASA under Contract No. NAS3-25368 and the NASA Graduate Student Researchers Program. Additional thanks are due to E. A. Winsa, D. C. Malarik, and their teams at NASA's Glenn Research Center at Lewis Field for their engineering design and support of the experiments.

[1] J. S. Langer, Rev. Mod. Phys. **52**, 1 (1980).
[2] *Dynamics of Curved Fronts*, edited by P. Pelcé, Perspectives in Physics (Academic, New York, 1988).
[3] M. E. Glicksman and S. P. Marsh, in *Handbook of Crystal Growth*, edited by D. T. J. Hurle (Elsevier, Amsterdam, 1993), p. 1077.
[4] D. Juric and G. Tryggvason, J. Comput. Phys. **123**, 127 (1996).
[5] U. Bisang and J. H. Bilgram, Phys. Rev. E **54**, 5309 (1996).
[6] M. E. Glicksman and S. C. Huang, in *Convective Transport and Instability Phenomena*, edited by Z. Karlsruhe and O. Karlsruhe (Publisher, City, 1982), p. 557.
[7] M. E. Glicksman, M. B. Koss, and E. A. Winsa, JOM **47**, 51 (1995).
[8] M. E. Glicksman, M. B. Koss, and E. A. Winsa, Phys. Rev. Lett. **73**, 573 (1994).
[9] M. E. Glicksman, E. A. Winsa, R. C. Hahn, T. A. LoGrasso, S. H. Tirmizi, and M. E. Selleck, Metall. Trans. A **19**, 1945 (1988).
[10] M. B. Koss, L. A. Tennenhouse, J. C. LaCombe, M. E. Glicksman, and E. A. Winsa, Metall. Trans. A (to be published, January, 2000).
[11] J. C. LaCombe, M. B. Koss, D. C. Corrigan, A. O. Lupulescu, L. A. Tennenhouse, and M. E. Glicksman, J. Cryst. Growth **206**, 331 (1999).
[12] E. Hürlimann, R. Trittibach, U. Bisang, and J. H. Bilgram, Phys. Rev. A **46**, 6579 (1992).
[13] V. K. Pinus and P. L. Taylor, J. Cryst. Growth **85**, 546 (1987).
[14] S.-C. Huang and M. E. Glicksman, Acta Metall. **29**, 717 (1981).
[15] B. Cantor and A. Vogel, J. Cryst. Growth **41**, 109 (1977).
[16] I. Steinbach, B. Kauerauf, C. Beckermann, and J. Gou (unpublished).
[17] J. S. Langer, Phys. Rev. A **36**, 3350 (1987).
[18] M. N. Barber, A. Barbieri, and J. S. Langer, Phys. Rev. A **36**, 3340 (1987).
[19] A. Barbieri, D. Hong, and J. S. Langer, Phys. Rev. A **35**, 1802 (1987).
[20] M. Ben-Amar and E. Brener, Phys. Rev. Lett. **71**, 589 (1993).
[21] E. Brener and D. Temkin, Phys. Rev. E **51**, 351 (1995).
[22] K. D. de Jager, Masters thesis, Rensselaer Polytechnic Institute, Materials Science and Engineering Department, 1996.
[23] J. C. LaCombe, M. B. Koss, V. E. Fradkov, and M. E. Glicksman, Phys. Rev. E **52**, 2778 (1995).
[24] A. Dougherty and A. Gunawardana, Phys. Rev. E **50**, 1349 (1994).
[25] Q. Li and C. Beckermann, Phys. Rev. E **57**, 3176 (1998).